

Dear Reviewer,

We appreciate your in-depth review of our manuscript and the important suggestions you provide for its submission. We have carefully considered the suggested changes and have tried our best to address each of your concerns within the manuscript and have outlined our justifications/ modifications below **point-by-point** (our responses are in bold). We strongly believe that your comments and suggested revisions have led to a much stronger and complete manuscript and would like to thank you again for the time and effort you put into reviewing this manuscript.

REVIEWER #1

Let me begin by saying that I believe this paper is a worthwhile contribution to this very interesting period in earth history, Middle Miocene Climatic Optimum, especially since this is a terrestrial record, and most records focus on marine. But I cannot recommend this for publication in its current state to *Climates of the Past*; however, I would happily rereview.

I have attached line by line comment in a pdf, but below I summarize my major concerns with the manuscript in its current format:

- I have some major concerns about how the carbonates and bulk geochemical samples were collected. These need to be collected from certain depths and it does not appear that they were. Things should also have been trenched and it does not appear that they were at least based on figure 2. I have made specific comments throughout the manuscript regarding these topics.

We agree that the field images provided gave the impression that samples were collected from the surface. However, we have provided new images which depict thick floodplain intervals that were sampled along with images depicting trenched samples collected below the weathering depth to avoid all signs of modern diagenesis and grain size.

Changes performed in MS:

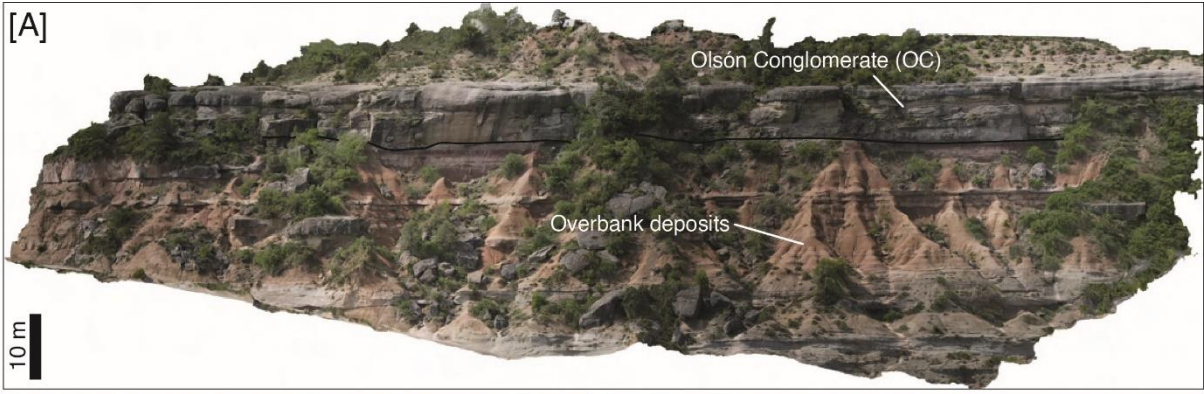
Line 76 – 97:

“The Escanilla Fm at Olsón has a maximum thickness of 1000 m and is subdivided into the Mondot and Olsón members (Figure 1C) (e.g., Labourdette & Jones, 2007). At the transition of these two members lies a basin-wide extending conglomeratic channel-complex, hereafter referred to as the Olsón Conglomerate (OC), which is the interpreted stratigraphic expression of peak MECO warming in the Escanilla Fm based on available age constraints (Figures 1B–1E). The Escanilla Fm predominantly consists of conglomeratic to sandy channel-fill deposits and their adjacent fine-grained floodplain/overbank deposits. These floodplain fines have been previously characterized as Entisols, displaying a low degree of pedogenesis (Dreyer et al., 1992). On the field, paleosols were identified based on pedogenic features such as horizonation, coloring, root

traces, and burrowing. In addition, we document the presence of three pedogenic carbonate nodule horizons (Figure 2C) and nine fluvial stromatolites preserved within the Escanilla floodplains (Figures 2D–2F). Although fluvial stromatolites are common in the upper Paleocene to Eocene fluvial deposits of Spain (Zamarreno et al., 1997), to our knowledge, they have not been identified in the Escanilla Fm before. These stromatolites have been preserved as elongated domes with an asymmetrical shape and have varying lengths from a few centimeters to a meter, and in diameter from 15 to 60 cm. They have been interpreted as having formed as overbank deposits of fluvial channels with a preferential elongation presumably parallel to the flow direction (Zamarreno et al., 1997). These stromatolites are also similar in appearance to Eocene stromatolites that grew on tree trunks from the Green River Formation, Colorado, USA (Awramik et al., 2015), although further research would be required to investigate this.

Within this context, a composite section of about 120 m was sampled for a suite of paleosol (ca. 200 g of fine-grained and fresh (unweathered) rock) and carbonate (pedogenic nodules and stromatolites) samples, collected below the weathering depth (at least 20 cm below modern surface) to avoid samples that could have been affected by diagenesis and may have altered grain size distribution (e.g., Lupker et al., 2011). Locations of sampled sites and corresponding raw data from different analyses have been provided as supplementary material.”

Line 121: Modified Figure 2.



Line 122 – 125: Modified caption of Figure 2.

“Figure 2. (A) Outcrop panorama depicting the Olsón Conglomerate (OC) and the thick floodplain interval sampled for paleosols. (B) Sampled paleosol. (C) Pedogenic carbonate nodules sampled below the weathering depth. (D) Long, tubular stromatolites (indicated by arrows) preserved in the floodplain. (E, F) Cross-section of stromatolite samples NS7 and NS1 respectively, showing the well-preserved individual layering. The white stars indicate micro-drilling sites.”

- None of the methods describe any efforts to identify or avoid diagenesis in the carbonates, such as petrography or cathodoluminescence.

We agree that no method to test for diagenesis was presented. To address this, we have included a new part titled ‘ Primary versus diagenetic signals’ in the results and discussion section. We have also addressed concerns regarding potential uncertainties involved in clumped isotope analysis.

Changes performed in MS:

Line 305 – 323: Added

“4.3 Primary versus diagenetic signals

Carbon and oxygen isotope composition of bulk paleosol carbonates may be affected by the diagenetic alteration of mineral phases. It is therefore important to evaluate the potential diagenetic overprint on primary geochemical signatures (e.g., [Marshall, 1992](#)).

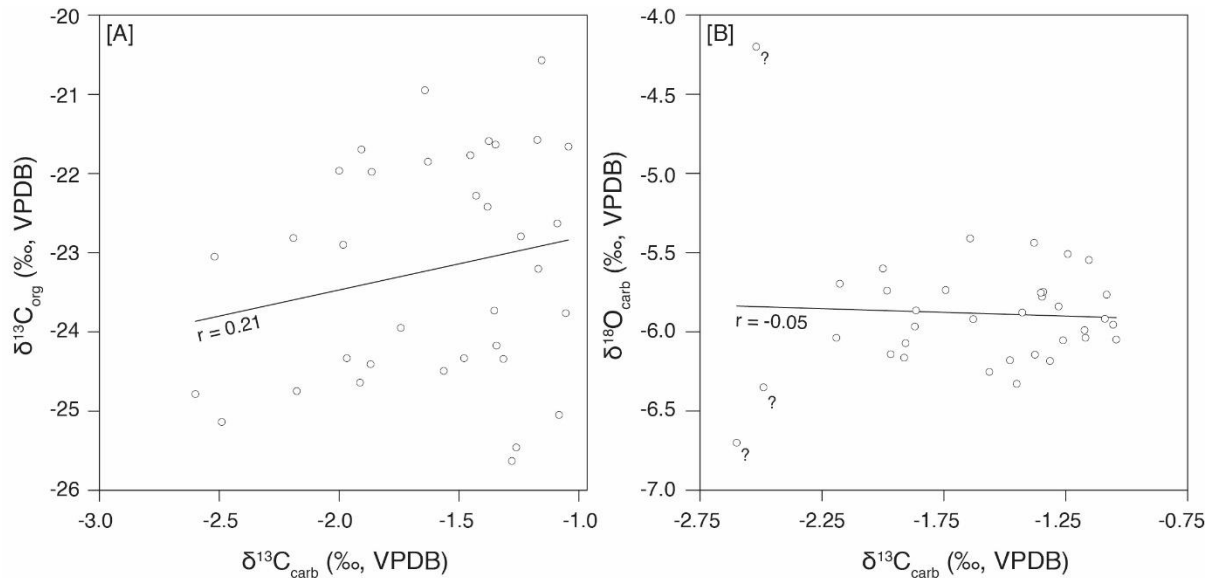
The degree of alteration was assessed through the relationship between $\delta^{13}\text{C}_{\text{org}}$ and $\delta^{13}\text{C}_{\text{carb}}$, and between $\delta^{18}\text{O}_{\text{carb}}$ and $\delta^{13}\text{C}_{\text{carb}}$ values. Pearson correlation coefficient, $r < 0.6$, indicates a statistically non-significant relationship and indicates that a diagenetic overprint on the primary signal can be excluded (e.g., [Fio et al., 2010](#)). In both correlation plots ([Figure 6](#)), no statistically significant correlation was found ($\delta^{13}\text{C}_{\text{carb}}$ vs $\delta^{13}\text{C}_{\text{org}}$: $r = 0.21$ ($P = .16$, $N = 45$), $\delta^{13}\text{C}_{\text{carb}}$ vs $\delta^{18}\text{O}_{\text{carb}}$: $r = 0.05$ ($P = .74$, $N = 45$)) indicating almost none or very minor diagenetic modification of the primary signal. Also, no correlation trend was observed between TOC and $\delta^{13}\text{C}_{\text{org}}$ (supplementary material; [Figure S1](#)).

Maximum Temperature (T_{max}) from rock eval analysis was used as a second approach to assess diagenetic alteration. T_{max} obtained in samples with high TOC (> 0.5 Wt. %) was < 440 °C which is the beginning of the oil window and indicates immature organic content (ca 60 °C, [Espitalié et al., 1985](#)).

As a third approach, paleosol samples (S9, S12, S17, S30) were analyzed using scanning electron microscopy (SEM). SEM images show presence of authigenic calcite (supplementary material, [Figures S2 – S4](#)), presence of authigenic clay minerals palygorskite and smectite (supplementary material, [Figures S5](#)) and detrital illite and

chlorite (supplementary material, [Figures S6](#)). Collectively, the three approaches suggest that the primary signal is largely preserved in the Escanilla Fm at Olsón.”

Line 324: Added Figure 6



Line 325 – 326:

“Figure 6. (A) Scatter plot of paleosol $\delta^{13}\text{C}_{\text{carb}}$ vs $\delta^{13}\text{C}_{\text{org}}$ values (B) Scatter plot of paleosol $\delta^{13}\text{C}_{\text{carb}}$ vs $\delta^{18}\text{O}_{\text{carb}}$ values. For both plots, Pearson correlation coefficient (r) and regression line is shown.”

Line 386 – 398:

“While measurement reproducibility was good, care must be taken while interpreting Δ_{47} data as a number of potentially significant uncertainties are associated with it. For instance, Δ_{47} temperatures may not necessarily reflect primary formation temperatures but could instead be the result of a combination of primary formation temperatures and secondary effects such as potential diagenetic temperatures that bias primary compositions, although secondary overprinting is unlikely to produce cooler temperatures ([Hren & Sheldon 2019](#)). Secondly, organic contaminants could cause Δ_{47} values to be variable although any volatile part would be discarded when the samples were dried at high temperatures overnight (70 to 80 °C). Third, more replicate measurements from the same homogenized powder are required to assess interference by contaminants in the drilled powders and to better constrain the spread in data. For preliminary data such as the one presented here, the mean value could be considered as a good temperature estimate. Finally, significant diagenetic alteration could cause Δ_{47} values to be variable although a similar temperature range in both stromatolites and

pedogenic nodules further suggests that analyzed samples most likely did not undergo significant diagenetic alteration after their formation. This would however need to be verified using petrography and/or cathodoluminescence.”

- Significant more attention needs to be paid to the literature about stromatolites and fluvial carbonates and the effects on carbon and oxygen isotopes that are very different than those that affect pedogenic carbonates.

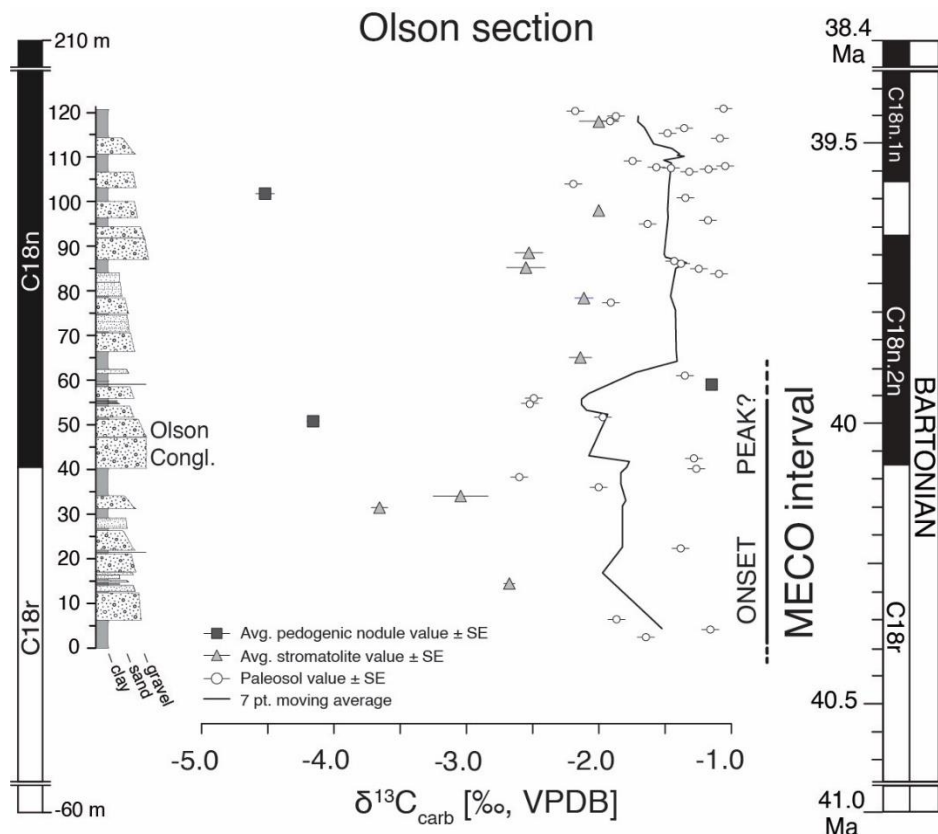
We agree that pedogenic carbonates and stromatolites form under completely different mechanisms. We have therefore presented the two datasets separately. Corresponding figures have also been modified accordingly with both datasets having different symbols.

Changes performed in MS:

Line 274 – 282:

“ $\delta^{13}\text{C}_{\text{carb}}$ values in stromatolites range from -3.9 ± 0.1 to -1.3 ± 0.1 ‰ with an average value of -2.5 ± 0.1 ‰ (N = 63, 5 to 9 replicate measurements from 9 sample horizons), while $\delta^{13}\text{C}_{\text{carb}}$ values in pedogenic nodules range from -4.9 ± 0.3 ‰ to -1.1 ± 0.3 ‰ with an average value of -3.2 ± 0.3 ‰ (N = 29, 9 to 10 replicate measurements from 3 sample horizons). Since sample size is limited stratigraphically, it does not permit a direct evaluation of the isotopic signal relative to the MECO. However, $\delta^{13}\text{C}_{\text{carb}}$ values from stromatolites and pedogenic nodules show a consistent 1 to 2 ‰ negative offset when compared to values from paleosol bulk carbonates, which is possibly due to the presence of detrital Mesozoic carbonates ($\delta^{13}\text{C}_{\text{carb}} = 0$ ‰; [Zamarreno et al., 1997](#)) in the bulk sediments from the source area.”

Line 282: Modified Figure 4.



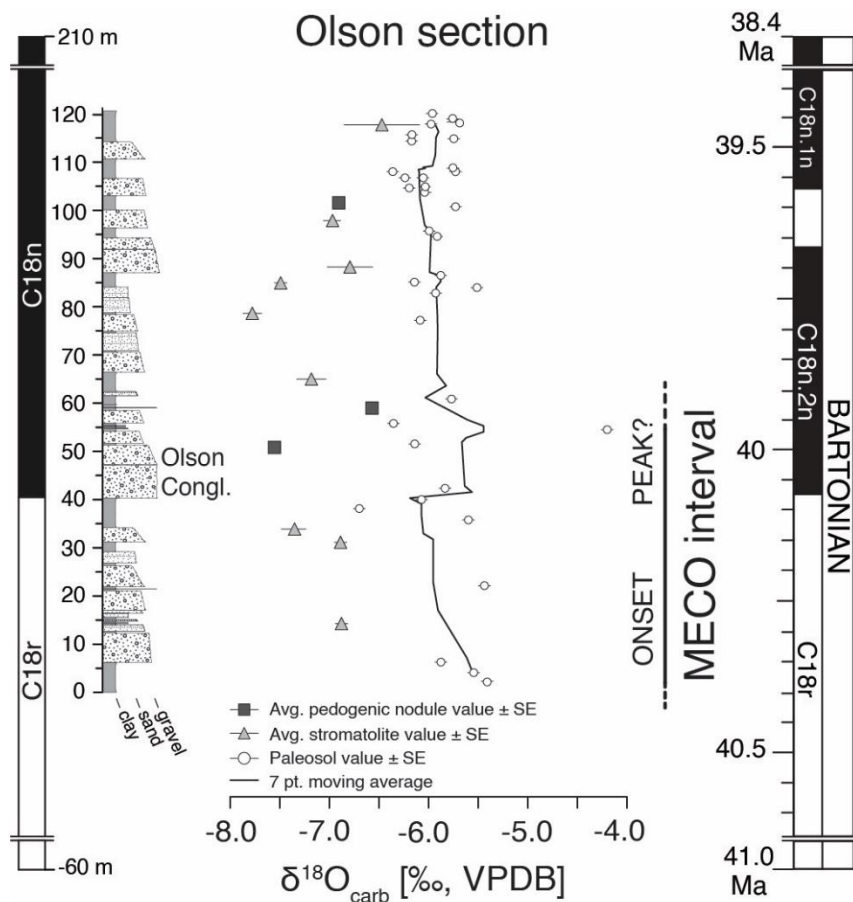
Line 283 – 285: Added

“Figure 4. Carbon isotope compositions ($\delta^{13}\text{C}_{\text{carb}}$) and associated standard error from paleosol bulk carbonates (white circles) with a 7-point moving average, and from stromatolite (triangles) and pedogenic nodules (squares) for the Olsón section. Also marked is the MECO onset and peak interval based on $\delta^{13}\text{C}_{\text{org}}$ values from this study.”

Line 293 – 295: Added

“ $d^{18}\text{O}_{\text{carb}}$ values in stromatolites range from -8.1 ± 0.1 to -4.7 ± 0.1 ‰ with an average value of -7.1 ± 0.1 ‰ (N = 63), while $d^{18}\text{O}_{\text{carb}}$ values in pedogenic nodules range from -7.6 ± 0.1 ‰ to -6.5 ± 0.1 ‰ with an average value of -6.9 ± 0.1 ‰ (N = 29); and crudely match the $d^{18}\text{O}$ -trend in paleosol bulk carbonates (Figure 5).”

Line 299: Modified Figure 5



Line 297 – 299: Added

“Figure 5. Oxygen isotope compositions ($\delta^{18}\text{O}_{\text{carb}}$) from paleosol bulk carbonates (white circles) with a 7-point moving average and associated standard error, and carbonate samples (stromatolites (triangles) and pedogenic nodules (squares)) for the Olsón section. Also marked is the MECO onset and peak interval based on $\delta^{13}\text{C}_{\text{org}}$ values from this study.”

Line 301 – 307:

“In summary, irrespective of the presence of authigenic and detrital carbonates in paleosol samples, the negative CIE in paleosol organic matter suggests that the MECO can be regionally recognized in the Escanilla Fm. Stable isotope data from the Escanilla Fm at Olsón is also compatible with climate perturbations through excursions similar to the isotope excursions in the marine records, even though there are differences in the magnitude of excursions. These excursions have also been identified downstream in the time-equivalent marine sediments in the Jaca Basin, Spain (Peris Cabré et al., 2023)

indicating the preservation of MECO climate perturbation signals in the source-to-sink Escanilla sediment routing system.”

- Many points in the discussion are unsupported by evidence either in the paper or from other literature. I noted areas that require more discussion or specificity to support these interpretations.

We agree that many points in the discussion were unsupported by evidence. We have carefully gone through all noted areas and supported our claims by citing relevant references or removed parts from the main text.

- The clumped isotope interpretations and analysis are lacking. More samples are needed to be able to make the interpretations in this paper. Some samples only have 1 replicate, which is not acceptable either for stromatolites or soil carbonates. In addition more attention needs to be paid to the literature for soil and stromatolite carbonates – reading some of this literature would really help to improve your interpretations.

While we agree that more clumped isotope analyses would help make stronger interpretations, currently available data has been presented as preliminary results and acknowledge that further research and analyses are required to evaluate the obtained trends.

Changes performed in MS:

Line 384 – 422: Modified entire section on carbonate clumped isotope thermometry

“4.5.2 Carbonate clumped isotope thermometry

Δ_{47} values of carbonate in stromatolites have a range from 0.634 to 0.704 ‰, translating into temperatures of 18 to 43 °C (Figure 8). Each stromatolite was analyzed 2 to 4 times for replicate measurements with standard error ranging from 0.006 to 0.011 ‰. Δ_{47} values of carbonate in pedogenic nodules have a range from 0.629 to 0.704 ‰, translating into temperatures of 18 to 45 °C (Figure 8). Each pedogenic nodule was analyzed 4 to 8 times for replicate measurements having standard error ranging from 0.006 to 0.009 ‰.

While measurement reproducibility was good, care must be taken while interpreting Δ_{47} data as a number of potentially significant uncertainties are associated with it. For instance, Δ_{47} temperatures may not necessarily reflect primary formation temperatures but could instead be the result of a combination of primary formation temperatures and secondary effects such as potential diagenetic temperatures that bias primary compositions, although secondary overprinting is unlikely to produce cooler temperatures (Hren & Sheldon 2019). Secondly, organic contaminants could cause Δ_{47}

values to be variable although any volatile part would be discarded when the samples were dried at high temperatures overnight (70 to 80 °C). Third, more replicate measurements from the same homogenized powder are required to assess interference by contaminants in the drilled powders and to better constrain the spread in data. For preliminary data such as the one presented here, the mean value could be considered as a good temperature estimate. Finally, significant diagenetic alteration could cause Δ_{47} values to be variable although a similar temperature range in both stromatolites and pedogenic nodules further suggests that analyzed samples most likely did not undergo significant diagenetic alteration after their formation. This would however need to be verified using petrography and/or cathodoluminescence.

Mean temperatures vary from 32.1 ± 1.8 °C to 38.6 ± 0.7 °C in the lower half of the section until 50 m followed by a peak mean temperature of 42 °C, just 25 m above the OC, without any observed change in lithology. Above 90 m until the top of the section, values return to an average value of 30 °C. Based on the available age constraints, our results suggest a potential lag between marine and terrestrial MECO climate signals. Our results also suggest a land-sea temperature gradient of 5 to 10 °C when compared to sea surface temperature (SST) records from ODP site 1172 (Tasmania, Pacific; [Bijl et al., 2010](#)), and IODP sites U1408 and U1410 (northwest Atlantic Ocean; [van der Ploeg et al., 2023](#)) most likely indicating an amplifying effect due to continentality. Similar continental temperature sensitivity during the Middle Eocene has also been previously identified through clumped temperatures of pedogenic carbonates in the continental interiors of SW Montana, USA ([Methner et al., 2016](#)). Further research and sample analysis would however be required to investigate this further.

Δ_{47} temperatures were further used to calculate the $\delta^{18}\text{O}$ of fluids in equilibrium with carbonates using the temperature dependent fractionation factor of [Epstein et al., \(1953\)](#). Δ_{47} temperatures and $\delta^{18}\text{O}_{\text{carb}}$ values in stromatolites give water d^{18}O values in the range of -5.9 to -2.1 ‰ (average of -3.3 ‰), while values from pedogenic nodules give water d^{18}O values ranging from -6.5 to -0.8 ‰ (average of -3.6 ‰) (data in supplementary material). For comparison, we also used the approach by [Kim & O'Neil \(1997\)](#), which gave water d^{18}O values from stromatolites to be in the range of -6.2 to -2.3 ‰ (average of -3.5 ‰) and -6.7 to -0.9 ‰ (average of -3.8 ‰) from pedogenic nodules (see supplementary material). These calculate water isotope values are consistent with meteoric water isotope composition at low latitude, but signify ^{18}O -isotope enrichment was most likely due to excess evapotranspiration under arid climatic conditions, consistent with estimates from other proxies used in this study.”

- Bulk carbonate should never be used in isotopic interpretations, it is too susceptible to diagenesis. Although it is useful to help determine IF your samples have diagenesis. See additional comments in text on this topic.

We agree that bulk carbonates are susceptible to diagenetic alteration. However, we would like to highlight that our regional identification of the MECO is based on a negative organic carbon isotope excursion and remains valid irrespective of whether detrital carbonates are present or not.

Changes performed in MS:

Line 301 – 302: Added

“In summary, irrespective of the presence of authigenic and detrital carbonates in paleosol samples, the negative CIE in paleosol organic matter suggests that the MECO can be regionally recognized in the Escanilla Fm.”

Line 305 – 323: Added

“4.3 Primary versus diagenetic signals

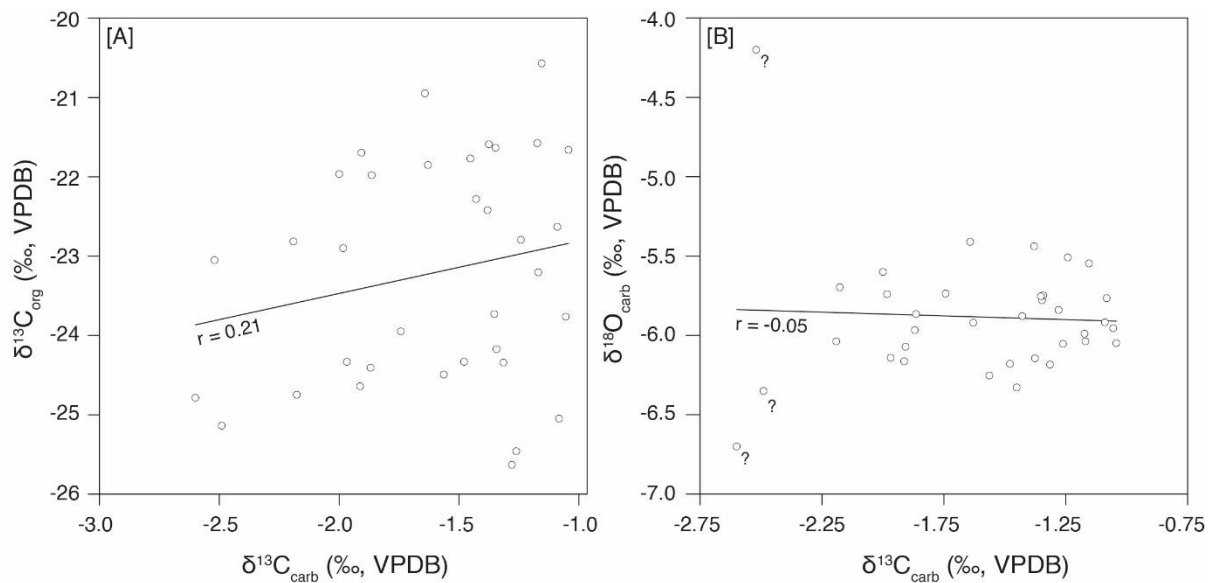
Carbon and oxygen isotope composition of bulk paleosol carbonates may be affected by the diagenetic alteration of mineral phases. It is therefore important to evaluate the potential diagenetic overprint on primary geochemical signatures (e.g., [Marshall, 1992](#)).

The degree of alteration was assessed through the relationship between $\delta^{13}\text{C}_{\text{org}}$ and $\delta^{13}\text{C}_{\text{carb}}$, and between $\delta^{18}\text{O}_{\text{carb}}$ and $\delta^{13}\text{C}_{\text{carb}}$ values. Pearson correlation coefficient, $r < 0.6$, indicates a statistically non-significant relationship and indicates that a diagenetic overprint on the primary signal can be excluded (e.g., [Fio et al., 2010](#)). In both correlation plots ([Figure 6](#)), no statistically significant correlation was found ($\delta^{13}\text{C}_{\text{carb}}$ vs $\delta^{13}\text{C}_{\text{org}}$: $r = 0.21$ ($P = .16$, $N = 45$), $\delta^{13}\text{C}_{\text{carb}}$ vs $\delta^{18}\text{O}_{\text{carb}}$: $r = 0.05$ ($P = .74$, $N = 45$)) indicating almost none or very minor diagenetic modification of the primary signal. Also, no correlation trend was observed between TOC and $\delta^{13}\text{C}_{\text{org}}$ (supplementary material; [Figure S1](#)).

Maximum Temperature (T_{max}) from rock eval analysis was used as a second approach to assess diagenetic alteration. T_{max} obtained in samples with high TOC (> 0.5 Wt. %) was < 440 °C which is the beginning of the oil window and indicates immature organic content (ca 60 °C, [Espitalié et al., 1985](#)).

As a third approach, paleosol samples (S9, S12, S17, S30) were analyzed using scanning electron microscopy (SEM). SEM images show presence of authigenic calcite (supplementary material, [Figures S2 – S4](#)), presence of authigenic clay minerals palygorskite and smectite (supplementary material, [Figures S5](#)) and detrital illite and chlorite (supplementary material, [Figures S6](#)). Collectively, the three approaches suggest that the primary signal is largely preserved in the Escanilla Fm at Olsón.”

Line 324: Added Figure 6



Line 325 – 326:

“Figure 6. (A) Scatter plot of paleosol $\delta^{13}\text{C}_{\text{carb}}$ vs $\delta^{13}\text{C}_{\text{org}}$ values (B) Scatter plot of paleosol $\delta^{13}\text{C}_{\text{carb}}$ vs $\delta^{18}\text{O}_{\text{carb}}$ values. For both plots, Pearson correlation coefficient (r) and regression line is shown.”

- I suggested some additional lines of research that should be investigated using the data you already have from bulk geochemistry PPM1.0, RF-MAP, mass balance, etc that would greatly improve your interpretations.

While we agree that the proposed additional lines of research would be beneficial, we have applied traditional methods widely used by the geochemistry community but would use the proposed methods in future studies.

Changes performed in MS: None

Detailed comments provided in the pdf have been addressed directly in the pdf and changes made to the manuscript have been listed below accordingly.

Changes performed in MS:

Line 81: ‘entisols’ changed to ‘Entisols’

Line 127 – 218: added detailed methods in the main text

“3 Material and methods

Analyses were carried out on a suite of sampled paleosols (N = 45), stromatolites (n = 9), and pedogenic nodules (n = 9 from 3 sample horizons) (Figure 1D). Pedogenic nodules were small and could not be cut open to be examined by cathodoluminescent microscopy or transmitted light. Hence, entire nodules were crushed, and their homogenized powders were used for analysis.

Powders of bulk paleosol samples were prepared and analyzed for geochemical indicators, including total organic carbon (TOC) content, Rock-Eval parameters, organic carbon isotope compositions ($\delta^{13}\text{C}_{\text{org}}$), carbonate carbon and oxygen isotopes ($\delta^{13}\text{C}_{\text{carb}}$ and $\delta^{18}\text{O}_{\text{carb}}$), major elements, and clay mineral assemblages. Stromatolite and pedogenic nodule powders were analyzed for $\delta^{13}\text{C}_{\text{carb}}$ and $\delta^{18}\text{O}_{\text{carb}}$ and clumped isotope compositions (d^{47} and D_{47}).

3.1 Rock eval analysis

Rock eval pyrolysis was performed at the Institute of Earth Sciences of the University of Lausanne (ISTE-UNIL) to assess the total organic carbon (TOC) content in the paleosols. The analyses were performed using a Rock-Eval 6 instrument, following the procedure described by Behar et al. (2001).

3.2 Organic carbon isotopes

The carbon isotope compositions of organic matter in paleosol samples were analysed in the stable isotope laboratories of the Institute of Earth Surface Dynamics, University of Lausanne (IDYST-UNIL). Samples first underwent de-carbonation with 10 % v/v HCl, then thoroughly washed with deionized water and dried at 40 °C for 48 h. The $\delta^{13}\text{C}_{\text{org}}$ measurements were made using a Carlo Erba 1100 (Fisons Instruments, Milan, Italy) elemental analyser connected to a Thermo Fisher Scientific Delta V Plus isotope ratio mass spectrometer, both operated under continuous helium flow. Measured $\delta^{13}\text{C}$ values were calibrated and normalized using international reference materials and in-house standards (Spangenberg 2006, 2016) and reported in per mil (‰) vs. Vienna Pee Dee Belemnite limestone standard (VPDB). The precision of the $\delta^{13}\text{C}_{\text{org}}$ values were better than 0.1 ‰.

3.3 Carbonate isotopes

Carbon and oxygen isotope compositions were determined at the IDYST-UNIL laboratories. Bulk paleosol samples containing >10 Wt.% CaCO_3 , including carbonate samples, were analysed using a Thermo Fisher Scientific Gas Bench II carbonate preparation device connected to a Delta V Plus isotope ratio mass spectrometer according to a method adapted after Spötl & Vennemann (2003). CO_2 gas was produced by reaction

with 99 % orthophosphoric acid at 70 °C. The $\delta^{13}\text{C}_{\text{carb}}$ and $\delta^{18}\text{O}_{\text{carb}}$ values are reported in ‰ vs. VPDB. Replicate measurements of the international calcite standard NBS 19 (limestone, $\delta^{13}\text{C} = +1.95$ ‰, $\delta^{18}\text{O} = -2.19$ ‰) and an in-house standard (Carrara marble, $\delta^{13}\text{C} = +2.05$ ‰, $\delta^{18}\text{O} = -1.7$ ‰) yielded an analytical precision (1σ) of ± 0.05 ‰ for $\delta^{13}\text{C}_{\text{carb}}$ and ± 0.1 ‰ for $\delta^{18}\text{O}_{\text{carb}}$.

3.4 Major elements

SiO_2 , Al_2O_3 , Fe_2O_3 , MnO , MgO , CaO , Na_2O , K_2O , P_2O_5 , Cr_2O_3 , NiO , and loss on ignition (LOI), were measured in the powdered bulk paleosol samples by X-ray fluorescence (XRF; Phillips PANalytical PW2400 spectrometer) at the ISTE-UNIL laboratories. The analyses were performed on fused glass discs prepared with 1.2000 ± 0.0005 g ignited sample powder and 6.0000 ± 0.0005 g of lithium tetraborate ($\text{Li}_2\text{B}_4\text{O}_7$). The concentrations of the major elements were expressed as Wt. % oxides. The analytical precision (1σ) assessed by replicate analyzed of international reference materials is 0.4 %.

3.5 Weathering indices

The chemical index of alteration (CIA in %; Eq. 1), proposed by Nesbitt & Young (1982), was used to quantify the degree of weathering by using the molar ratio of immobile Al_2O_3 and the mobile oxides CaO , Na_2O , and K_2O in the silicate fraction (e.g., Deng et al., 2022). The CIA is commonly used to estimate the intensity of alteration and test for environmental factors (e.g., temperature, precipitation, elevation, slope) affecting silicate weathering.

$$CIA = \frac{\text{Al}_2\text{O}_3}{\text{Al}_2\text{O}_3 + \text{Na}_2\text{O} + \text{CaO}^* + \text{K}_2\text{O}} \times 100 \quad (1)$$

, where CaO^* is the CaO incorporated in the silicate fraction and is calculated as:

$$\text{CaO}^* = \text{CaO} - [(10/3) \times \text{P}_2\text{O}_5] \quad (2)$$

Intense weathering removes mobile oxides, concentrating Al_2O_3 to a maximum value of almost 100 Wt.%; whereas weak weathering would give lower CIA values (<50 %) because of dominance of mobile oxides.

For comparison to the CIA, we used the chemical index of weathering (CIW in %; Eq. 3) proposed by Harnois, (1988), which is a modified version of the CIA to account for potassium metasomatism in paleosols during weathering (Stein et al., 2021) (See supplementary material, Figure S7).

$$CIW = \frac{\text{Al}_2\text{O}_3}{\text{Al}_2\text{O}_3 + \text{Na}_2\text{O} + \text{CaO}^*} \times 100 \quad (3)$$

, where CaO^* is the CaO incorporated in the silicate fraction (Eq. 2).

3.6 Mean annual precipitation

Mean annual precipitation (MAP) was estimated from the CIW (Eq. 4; standard error = $\pm 182 \text{ mm yr}^{-1}$) using the equation proposed by [Sheldon et al. \(2002\)](#) as:

$$MAP = 221e^{0.0197(CIW)} \quad (4)$$

3.7 Clumped (Δ_{47}) isotopes

Clumped isotope compositions were measured at the IDYST-UNIL laboratories, using a Nu Perspective dual-inlet mass spectrometer with an automated NuCarb sample preparation device. Carbonate digestion, CO₂ purification procedure, and measurements followed [Anderson et al. \(2021\)](#). For Δ_{47} analyses, 3.8 to 4.2 mg of carbonate were reacted at 70 °C with 110 μl 105 Wt.% phosphoric acid (H₃PO₄), and the liberated CO₂ was purified after digestion in a series of temperature-controlled, liquid-nitrogen-cooled cold fingers, including an adsorption trap (packed with Porapak Q 50/80 mesh) held at -30 °C. We applied the acid fractionation factor of +0.088 ‰ ([Anderson et al., 2021](#)) to the data in order to compare with the ETH-standards reacted at 90 °C ([Bernasconi et al., 2021](#)).

Three standards (ETH-1, ETH-2, ETH-3) have been used to calculate Δ_{47} values of unknown samples using linear regression with the respective Δ_{47} values of 0.205, 0.209, and 0.613 ([Bernasconi et al., 2021](#)). Temperatures are calculated using the calibration of [Anderson et al. \(2021\)](#), where Δ_{47} is in ‰ and T in °C, as:

$$\Delta_{47} = (0.0391 \pm 0.0004) \times (10^6/T^2) + (0.154 \pm 0.004)$$

Multiple analyses were carried out on the drilled powders of eachstromatolites (n = 2 to 4) and pedogenic nodules (n= 4 to 8) samples, to obtain better statistics (data in supplementary material).

3.8 Clay mineralogy

Clay mineralogical assemblages in paleosol samples were determined by X-ray diffractometry (XRD) at the ISTE-UNIL laboratories. Samples were prepared following the procedure described in [Adatte et al. \(1996\)](#). Analyses were made using a Thermo Fisher Scientific ARL X-TRA diffractometer and the intensities of the XRD peaks characteristic of each mineral, were used to estimate the relative percentage in bulk rock and < 2 μm and 2–16 μm clay size fractions.

3.9 Uncertainty on reported data

All data reported in this study is associated with uncertainties in the form of standard error of the mean (SE) calculated as $SE = \frac{SD}{\sqrt{n}}$, where SD is the standard deviation and n is the number of replicates analyzed. Uncertainty propagation was done using the

uncertainties package on Python (Spyder 4.0.1), which is an open-source and cross-platform program that handles calculations with numbers involving uncertainties.”

Line 221 – 236: Modified discussion of $\delta^{13}\text{C}_{\text{org}}$ data

“4.1 TOC content and $\delta^{13}\text{C}$ of bulk paleosol organic matter

TOC content in paleosol samples varies from 0.01 ± 0.01 to 0.57 ± 0.01 Wt. % with an average value of 0.07 ± 0.01 Wt. % (N = 45) (Figure 3). Low TOC may be indicative of low primary productivity, in this case ‘vegetation’ including grasses and higher plants, and (cyno)bacteria or low preservation of organic matter due to an oxidizing (oxygenated) environment (Tyson, 1995).

The $\delta^{13}\text{C}_{\text{org}}$ values of the paleosols have a range between -26.0 ± 0.2 and -20.4 ± 0.2 ‰ with an average value of -23.2 ± 0.2 ‰ (N = 45) (Figure 3). A negative CIE is marked by a 3 ‰ shift from the base of the section (from 0 to 30 m), where the onset begins, followed by a plateau of low values (30 to 50 m) that gradually return to higher values 60 m upwards. This negative CIE is most likely coeval to the 0.5 ‰ negative excursion observed in the benthic foraminifera $\delta^{13}\text{C}_{\text{cib}}$ values from ODP sites 738 (Bohaty et al., 2009) (Figure 3), indicating a general agreement in the change of $\delta^{13}\text{C}$ values, even though absolute differences in the magnitude of excursions exist.

A similar large magnitude negative CIE was previously identified for the PETM within the intermontane Piceance Creek Basin of western Colorado (USA), where a negative CIE of about 3 ‰ was reported (Foreman et al., 2012). The $\delta^{13}\text{C}_{\text{org}}$ record from the Middle Eocene Alano di Piave section deposited in the marginal Tethys Ocean recorded a negative CIE of about 1 ‰ (Spofforth et al., 2010) while the coeval shallow water Sealza section from Italy recorded a negative CIE of 2 ‰ (Gandolfi et al., 2023).”

Line 242 – 253:

“The $\delta^{13}\text{C}_{\text{org}}$ values can also be used as indicators of paleoecology and paleoclimate (Kohn, 2010). C_3 plants which include trees, most shrubs and cool season grasses, have $\delta^{13}\text{C}$ values between -37 ‰ and -20 ‰ and have dominated the history of terrestrial vegetation (Kohn, 2010). This wide range in $\delta^{13}\text{C}$ values of plants is dependent on several factors such as temperature, altitude, latitude, and MAP (Schulze et al., 1996; Kohn, 2010). Non water-stressed C_3 plants are enriched in ^{12}C and hence have more negative $\delta^{13}\text{C}$ values, typically lower than -26 ‰. Higher $\delta^{13}\text{C}$ values (> -26 ‰) are associated with plants growing under water deficient conditions and low soil transpiration rates (MAP < 500 mm yr^{-1}) (e.g., Cerling & Quade 1993; Kohn, 2010; Methner et al., 2016). Measured $\delta^{13}\text{C}_{\text{org}}$ values suggest a predominance of C_3 vegetation, consistent with an Eocene ecosystem (Cerling & Quade 1993; Methner et al., 2016). A significant proportion of measured values have relatively high $\delta^{13}\text{C}$ values (> -23 ‰) that are characteristic of dry environments with MAP < 500 mm yr^{-1} (Kohn, 2010). Low primary productivity and low

organic matter preservation complemented by elevated $\delta^{13}\text{C}_{\text{org}}$ values likely indicates sparse vegetation in a dry and arid ecosystem.”

Line 332 – 335: Added

“CIA values range from 9 ± 1 to 43 ± 1 % with an average value of 19 ± 1 % (N = 45). A slight peak in CIA values may represent peak weathering conditions during the MECO (Figure 7). CIA values have further been compared to CIW values (supplementary material; Figure S7), which takes into account potassium metasomatism, which range from 10 ± 1 to 48 ± 1 % with an average value of 20.5 ± 1 % (N = 45).”

Line 339 – 342: Added

“Our relatively low CIA values at Olsón could be related to the long-term trend of low silicate weathering in response to elevated $p\text{CO}_2$ and warming levels during the Middle Eocene as indicated by osmium isotopes (van der Ploeg et al., 2018) and more recently by lithium isotope data available from the marine environment (Krause et al., 2023).”

Line 358 – 378: modified presentation and discussion of MAP results

“MAP values in the Olsón section range from 270 ± 10 to 570 ± 10 mm year⁻¹ with an average of 330 ± 10 mm year⁻¹. Values stay constant at 300 ± 10 mm year⁻¹ until 40 m followed by a 20 % increase in precipitation, up to 370 ± 10 mm year⁻¹, which most likely corresponds to the OC (peak MECO conditions). Above the OC, MAP values return to an average value of 340 ± 10 mm year⁻¹ until the top of the section (Figure 8). Overall, these values predict arid to semi-arid climate in this area of the southern Pyrenees during the Middle Eocene and are coherent with the high $\delta^{13}\text{C}_{\text{org}}$ values (water-stressed environments), low CIA and CIW values (diminished chemical weathering) in our section. At Igualada in the Ebro Basin, 200 km away from Olsón, palynological, pollen taxa and floral diversity studies suggest warm climate and humid vegetation, with preservation of mangrove swamp vegetation along the coast (Cavagnetto and Anadón 1996; Haseldonckx, 1972). The absence of humid climate in Olsón could be due to its location being higher in elevation and away from the coastline as compared to Igualada. Such regional differences in climate could also be the result of a climate transition phase during the Middle Eocene, oscillating from a warm tropical Early Eocene to a cold and arid Early Oligocene, expressed differently in different regions and at possibly different sampled intervals.

MAP estimates based on well-dated megaflores from the Weissensteiner and Lausitz Basins (both in northeast Germany), consisting of shallow marine and continental deposits, are in the range of 1100 to 1400 mm year⁻¹ (Mosbrugger et al., 2005). Other proxy data from southern France indicate a MAP less than 500 mm year⁻¹ in the Bartonian (Kocsis et al., 2014), and is similar to our calculation from Spain. In conclusion, the values reported

here should be regarded as being representative of a local signal, most likely influenced by rainshadow effects imposed by the Pyrenean topography at that time, which rose to 2000 meters between 49 and 41 Ma (Huyghe et al., 2012), thus possibly inducing orographic effects as observed in the modern situation (Vacherat et al., 2017; Huyghe et al., 2018).”

Line 386 – 398: Added discussion on uncertainties associated with clumped isotope data.

“While measurement reproducibility was good, care must be taken while interpreting Δ_{47} data as a number of potentially significant uncertainties are associated with it. For instance, Δ_{47} temperatures may not necessarily reflect primary formation temperatures but could instead be the result of a combination of primary formation temperatures and secondary effects such as potential diagenetic temperatures that bias primary compositions, although secondary overprinting is unlikely to produce cooler temperatures (Hren & Sheldon 2019). Secondly, organic contaminants could cause Δ_{47} values to be variable although any volatile part would be discarded when the samples were dried at high temperatures overnight (70 to 80 °C). Third, more replicate measurements from the same homogenized powder are required to assess interference by contaminants in the drilled powders and to better constrain the spread in data. For preliminary data such as the one presented here, the mean value could be considered as a good temperature estimate. Finally, significant diagenetic alteration could cause Δ_{47} values to be variable although a similar temperature range in both stromatolites and pedogenic nodules further suggests that analyzed samples most likely did not undergo significant diagenetic alteration after their formation. This would however need to be verified using petrography and/or cathodoluminescence.”

Line 425 – 447: Modified presentation and discussion of clay mineralogy data

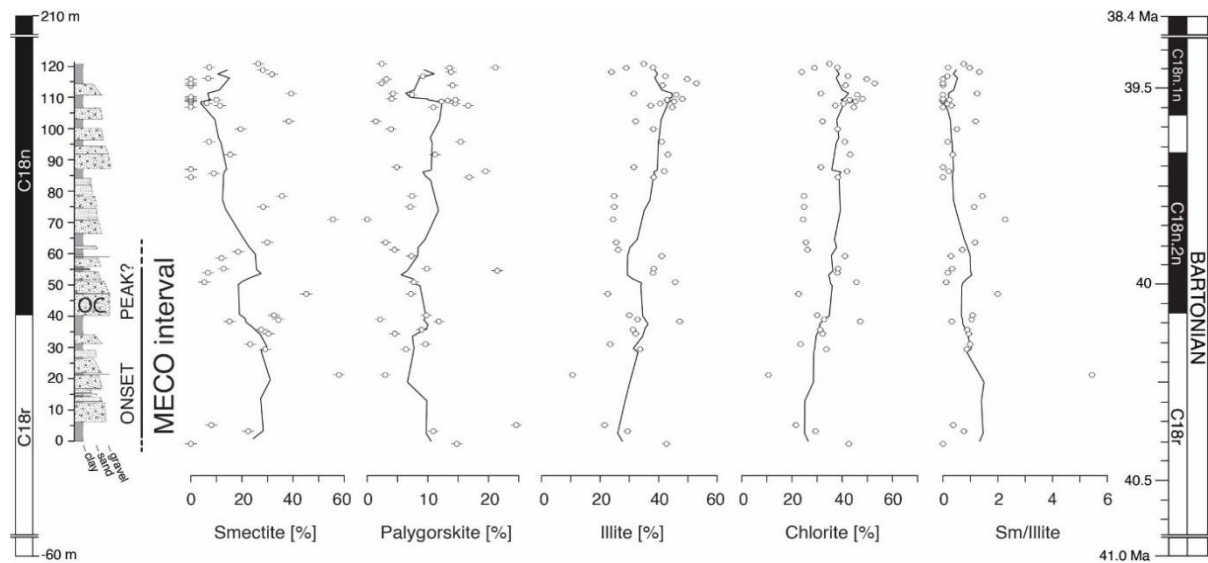
“Clay mineral assemblages in paleosols are also important paleoclimatic indicators and reflect detrital mineral input, composition of the source area lithology, type of weathering of the source rocks, to provide integrated records of the overall climate (Singer 1984; Franke & Ehrmann 2010; Rego et al., 2018).

Smectite, palygorskite, illite, and chlorite form up to 98 % of the identified mineral assemblages in the studied section (Figure 9). Smectite, commonly derived from alteration of volcanic rocks, forms under seasonal rainfall conditions with a pronounced dry season (e.g., Singer, 1984; Tabor et al., 2014) and constitutes on average 17 % of the total identified clay mineral assemblage while individual values reach up to 58 %. Palygorskite, an authigenic mineral (supplementary material, Figure S5), is indicative of an arid to semi-arid environment where evapotranspiration exceeds precipitation (e.g., Birkeland, 1984; Singer, 2002; Meunier, 2005), and constitutes up to 25 % (average of 10 %) of the total clay mineral assemblage. Illite content is between 11 and 53 % (average of 36 %), while chlorite content is between 7 to 64 % (average of 35 %) in the analyzed

paleosols. High amounts of illite and chlorite, both detrital minerals (supplementary material, [Figure S6](#)), are typically found in sediments formed by physical erosion of low-grade metamorphic rocks and are thus indicative of weak, incipient chemical weathering ([Tabor et al., 2014](#); [Rego et al., 2018](#)), and support our calculated CIA values. Except for palygorskite, clay mineral variations can be inferred to reflect weathering conditions in the source area of the Escanilla sediment routing system.

Increase in authigenic palygorskite content above the OC indicates environmental conditions on land became drier which is in agreement with previous studies showing an increase in aridification following the MECO interval in NW China ([Bosboom et al., 2014](#)) and in the Neo-Tethys (Baskil section, eastern Turkey; [Rego et al., 2018](#)). This is also in agreement with our decreasing smectite/illite ratios above the OC ([Figure 9](#)) and is consistent with values reported by [Rego et al. \(2018\)](#). Overall, interpretation of clay mineral assemblages corroborates well with environmental conditions deduced from organic carbon stable isotopes data, weathering indices and mean annual precipitation.”

Line 448: Added new Figure 9 to display clay mineralogy data



Line 449 – 452: Caption of Figure 9

“Figure 9. Identified clay mineral assemblages (smectite, palygorskite, illite, chlorite) and smectite/illite ratios are presented with respective standard error values and a 7-point moving average (black line) across the studied Escanilla Formation at Olsón. These minerals constitute up to 98% of the total clay mineralogy and suggest the presence of an arid to semi-arid climate under weak chemical weathering conditions during the MECO in the southern Pyrenees, Spain.”

Line 455 – 465: Modified Conclusions

“Detailed geochemical and mineralogical analysis of paleosols, stromatolites, and pedogenic nodules, provides new insights into terrestrial records of the MECO in the Ainsa Basin of the southern Pyrenees, Spain. A negative CIE measured on organic matter indicates the local preservation and identification of the MECO in the fluvial Escanilla Fm demonstrating that continental sedimentary successions can serve as important climate archives and highlighting stable isotope proxies as a powerful dating and correlation tool in notably difficult-to-date fluvial successions. Low CIA values in the Escanilla Formation suggest poor silicate weathering feedback in response to elevated pCO₂ levels and a prevalence of physical erosion during the Middle Eocene. This is compatible with an arid to semi-arid climate with a locally diminished hydrological cycle, as supported by low MAP estimates and identified clay mineral assemblages in the fluvial sedimentary succession. Carbonate clumped isotope thermometry suggests high temperatures up to 42 °C and a possible amplifying effect of 10 to 15 °C on continents compared to temperature records from the deep sea.”